Orientation-dependent conductance study of pentacene nanocrystals by conductive atomic force microscopy

Wei-Shan Hu,[1,2] Yu-Tai Tao,[1,2,a)] Yen-Fu Chen,[3] and Chia-Seng Chang[3]
[1]*Institute of Chemistry, Academia Sinica, Taipei 115, Taiwan*
[2]*Department of Chemistry, National Tsing Hua University, Hsinchu 300, Taiwan*
[3]*Institute of Physics, Academia Sinica, Taipei 115, Taiwan*

(Received 19 February 2008; accepted 27 June 2008; published online 6 August 2008)

Oriented pentacene nanocrystals with long molecular axis either parallel or perpendicular to a Au substrate were prepared on a bare Au surface or a self-assembled monolayer (SAM)-modified Au surface, respectively. The conductance across the differently oriented pentacene crystals were measured by conductive atomic force microscopy in a similar device configuration of Au/SAM/pentacene/Au-tip and Au/pentacene/SAM-modified-Au-tip, respectively. Rectifying current was observed depending on the location of the SAM in the device. With an average thickness of 50 nm, the conductance along the C–H$\cdots\pi$ stacking direction (*a*-*b* plane) was nearly five orders of magnitude larger than along the layer direction (*c* axis). © *2008 American Institute of Physics*. [DOI: 10.1063/1.2960343]

The understanding of intrinsic charge transport property of an organic semiconducting crystal is crucial for using such material in fabricating efficient electronic devices such as organic thin film transistors, organic light-emitting diodes, organic solar cells, etc. The charge transport in a molecular crystal has in general been suggested and, in some cases, measured to be anisotropic, due to different electronic interactions between neighboring molecules along different directions in a three-dimensional, orderly packed framework.[1] Pentacene is one of the most prominent organic channel materials for transistor application, with its field-effect mobility rivaling that of amorphous silicon. In pentacene single crystal, the molecules pack into layers with herringbone arrangement of neighboring pentacenes within the layers due to the preferred C–H$\cdots\pi$ interactions. Theoretical calculations concluded that the charge transport in pentacene single crystal has a dominant two-dimensional character and takes place mainly within the *a*-*b* planes due to a significant electronic coupling along the *a* axis and the *d*1 and *d*2 axes. The coupling between molecules located in adjacent layers (that is, along the *c* axis) is negligible.[2] However, direct measurement of charge conduction across layers (*c* axis) has not been reported.

The anisotropic character in charge conduction means alignment of pentacene crystals relative to the source/drain electrodes is important when a thin film pentacene is used as the conduction channel. The alignments of organic molecules with respect to a substrate surface by different methods have been documented.[3] Our previous study has shown that pentacene molecules initially deposited on a bare Au surface will adopt planar adsorption geometry, which induces a crystal growth with the long molecular axes of pentacene molecules lying parallel to the substrate.[4] The strong interaction between π-electron cloud of pentacene and the empty orbitals of Au can nevertheless be blocked by a preadsorbed self-assembled monolayer (SAM) of organic thiolate molecules and a layered crystal structure is resulted, with the long molecular axes of pentacenes oriented near perpendicular to the SAM-modified gold surface. The differently oriented pentacene crystals on a bare Au surface and a SAM-modified Au surface offers the opportunity of probing the charge transporting property through different directions of crystalline pentacene.

Conductive atomic force microscopy (CAFM) and scanning tunneling microscopy have been used to study electrical properties of materials in nanoscale.[5] Topographic images and electrical measurements can be collected at the same time to pinpoint the electric properties of a specific area.[6–8] Electric force microscopy (EFM) is another powerful tool for studying inhomogeneous charge trapping in pentacene thin film and ambipolar charge injection in a single pentacene monolayer island.[9] In this letter, we report the conduction behaviors of highly oriented pentacene nanocrystals by using CAFM. Differently oriented pentacene nanocrystals were prepared simultaneously on a SAM-patterned Au surface by thermal evaporation. The *I*-*V* response was measured across a specific crystalline grain between the Au substrate and the CAFM tip. The EFM was applied to show the different phase responses of the patterned areas in the presence of an electric field, as a result of different electric conductance of the pentacene films.

The gold substrate was prepared by evaporating 130 nm high purity (99.99%) gold from a resistively heated tungsten boat onto a silicon (100) wafer primed with 13 nm chromium. A hard poly(dimethylsiloxane) stamp[10] for microcontact printing was inked with an ethanolic solution of 1 mM biphenyl-4-thiol and brought into contact with a gold surface for 2 min and then the resulting substrate was thoroughly rinsed with pure EtOH and dried with a stream of nitrogen. The deposition of pentacene was carried out in a vacuum chamber, with the substrate kept at room temperature, at an evaporation rate of 1 Å/s under a pressure of 2×10^{-5} torr. AFM measurements were carried out under ambient conditions using a Digital Instruments Nanoscope III microscope operated in tapping mode. CAFM measurements were carried out under ambient conditions using Asylum Research MFP-3D AFM connected with an Agilent 4156C Precision Parameter Analyzer equipped with a close loop (PIS loop) control to eliminate the influence of electrostatic force during

a)Tel.: +886-2-27898580. FAX: +886-2-27831237. Electronic mail: ytt@chem.sinica.edu.tw.

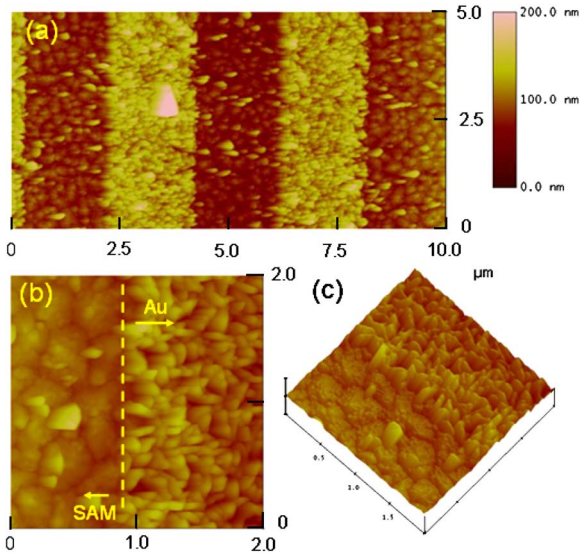

FIG. 1. (Color online) AFM images of 50-nm-thick pentacene films on biphenyl-4-thiol-patterned Au surface. (a) 5×10 μm^2, (b) 2×2 μm^2, and (c) 3D image.

measurement. The conductive Au-coated tip (from Micromasch, Russia) had a 20 nm Au film with a 20 nm Cr underlayer. The coated tip had a curvature radius less than 50 nm. A SAM-modified tip was formed by soaking the Au-coated tip in a 1 mM solution of biphenyl-4-thiol in ethanol for 20 min before rinsing with ethanol and blowing dry with N_2.

The AFM images of 50 nm pentacene film deposited on a SAM-patterned Au surface are shown in Fig. 1. Patterns of parallel strips with a width of 2 μm can be seen on the SAM-modified Au surface. Zooming in the image [Fig. 1(b)] reveals different morphologies on different areas: the thicker areas consist of randomly distributed rod-shaped grains, with many voids and spaces exist between the grains. Whereas for the thinner area, the film is smoother with rather large island-like and tightly packed grains of layered structure. In consistency with our earlier report,[4] the thicker areas are assigned as pentacene deposited on bare Au surface. The molecules in the grains have their long molecular axes parallel to the Au surface. The thinner and smoother areas are assigned as pentacene deposited on the SAM-modified areas. The molecules in these grains have their long molecular axes oriented near perpendicular to the surface. The different morphologies resulted from different growth rates along different crystalline planes: faster in the *a-b* plane due to the C–H$\cdots\pi$ interactions and herringbone packing of the molecules but slower in the *c* axis that defines the layer direction. Figure 1(c) shows the three-dimensional (3D) image of the border area.

The *I-V* characteristics across the pentacene film were measured by conductive AFM. After the topography image was captured by tapping mode, the CAFM tip was brought into contact with a specific grain for *I-V* measurement. The force applied between the tip and the pentacene grain during the measurement was monitored by the controller. Figure 2(a) shows the *I-V* curves obtained on a grain of pentacene deposited on the SAM-modified Au surface, with the topography image of the pentacene film included in the inset. The red dot in the AFM image indicates the point contacted by the Au-coated tip. The force applied between the tip and the crystal was 100 nN. Au substrate was connected to the ground and the tip was applied with bias sweeping from −2 to 2 V. *I-V* curves numbered from 1 to 5 in Fig. 2(a) show different scans measured on the same spot. The curves were reproducible and exhibited a rectifying behavior. A current of $\sim4\times10^{-9}$ A was recorded at a bias of +2 V. Scan number 6 shows the *I-V* trace with the tip withdrawn away from the sample surface, where no current was measured. Direct measurement with the Au-coated tip on a pentacene grain deposited on bare Au surface resulted unstable and irreproducible currents. However, when the Au-coated tip was modified with the same biphenyl-4-thiol SAM, reproducible *I-V* curves were observed, as shown in Fig. 2(b). A rectifying behavior was again observed, with a negative current up to 10^{-4} A at a tip bias of −2 V. It should be noted that the configurations of the devices were the same for the two measurements, arranged only in opposite direction. Another difference was the packing orientation of the pentacene molecules between the electrodes: layers of perpendicularly oriented molecules in one and flat-lying molecules in herringbone arrangement in the other. The currents differ by a factor of $\sim10^5$. It is noted that the apparent thickness of the two crystals were different. Still, a higher current was measured for the thicker film. Thus a factor of 10^5 should be the lower limit of the difference for grains of similar thickness. When the *I-V* measurement was carried out on a device with symmetric layout, i.e., SAM-modified Au-tip/50 nm pentacene/SAM-modified-Au-surface, currents were observed in either bias [Fig. 2(c)], with nonsymmetrical current response, which is suggested to be due to the nonsymmetric placement of Fermi level of the electrode relative to the highest occupied molecular orbital/lowest unoccupied molecular orbital (HOMO/LUMO) levels (see below).

The rectifying behavior shown in Fig. 2 can be rationalized as the following. When the tip makes contact with the organic surface, a Schottky barrier forms and the applied bias

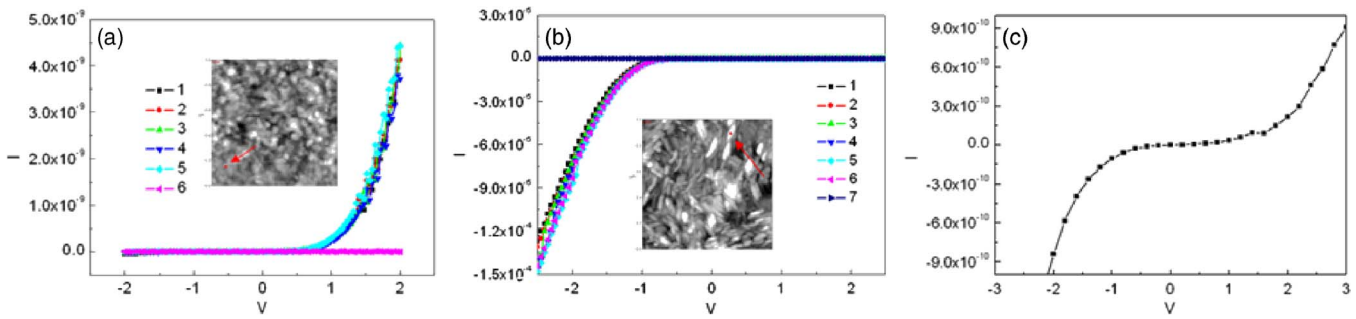

FIG. 2. (Color online) *I-V* characteristics of 50-nm-thick pentacene grain on (a) biphenyl-4-thiol SAM-modified Au surface using Au-coated tip; (b) on bare Au surface using biphenyl-4-thiol SAM-modified Au tip; (c) on SAM-modified Au surface using SAM-modified Au tip. The insets show 1×1 μm^2 AFM image of pentacene film, with the red dot indicating the spots for *I-V* measurement.

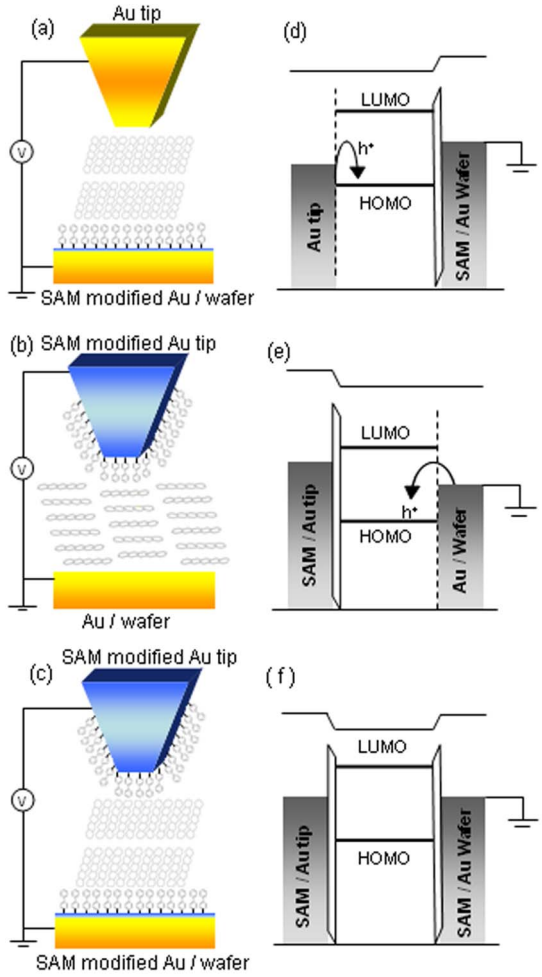

FIG. 3. (Color online) Schematic representations of CAFM measurement geometry of (a) Au tip/pentacene deposited on SAM-modified Au wafer; (b) SAM-modified Au-tip/pentacene deposited on bare Au wafer; (c) SAM-modified Au-tip/pentacene deposited on SAM-modified Au wafer. (d) The energy-level alignments of devices in (a), (b), and (c), respectively.

voltage drops mainly within the organic layer. The energy level alignments are similar to that of a single-layer organic light emitting diode.[11] The work function of the electrode determines the efficiency of electron and hole injection into the organic layer. The dipole moment and its direction associated with a self-assembled monolayer serve to tune the metal work function and, thus, the charge injection in the optoelectronic device.[12] For Au electrode modified by a SAM of biphenyl-4-thiol, the work function is expected[13] as well as measured to be lowered (from 5.08 to 4.46 eV). Different injection barriers result in the rectifying behavior observed. Figures 3(a)–3(c) display the schematic representations of three device configurations, with the corresponding energy-level alignments shown in Figs. 3(d)–3(f). It is noted that the HOMO levels for pentacene oriented differently on gold were measured to be different, with flat-lying pentacene having a HOMO located −1.35 eV from the Fermi level of Au and vertical pentacene having a HOMO located −0.95 eV from the Fermi level.[14]

Electrostatic force microscopy was carried out on a 50-nm-thick pentacene film deposited on a biphenyl-4-thiol-patterned Au surface. After the topography image of the film was taken, the tip was lifted up to 150 nm above the surface and the same trace of topography scan was followed, at different applied bias on the tip. At 0 V bias, no difference in phase contrast was observed over the same patterned area. However, when a tip bias of 10 V was applied, pentacene on the bare Au areas showed lower phase response than that on the SAM-modified areas. The phase lag in the pentacene films on the bare Au areas is due to stronger electrostatic forces, which originate from better conductivity for pentacene films in these regions. Similar image was obtained with a tip bias of −10 V.

In conclusion, the conductance across highly oriented pentacene nanocrystals was measured to be strongly dependent on the packing orientation. With an average thickness of 50 nm of pentacene grain, the charge transport through the $C-H\cdots\pi$ stacking direction (the *a-b* plane of pentacene crystal) is nearly five orders of magnitude higher than that along the layered *c* direction.[15] Current rectification was observed in a device configuration of Au/SAM/pentacene/Au due to change of the work function after SAM modification. The large difference in conductance is attributed to the weak electronic coupling between layers of pentacene, plus different electrode contact and, thus, contact resistance. Considering the report that pentacene molecule coordinates perpendicularly on Au has lower injection barrier than pentacene lying flat on Au,[14] this would mean the current difference measured is only a lower limit originating from different electronic coupling along the *a-b* direction and *c* direction. In summary, the results point to the importance of understanding and controlling the molecular orientation in an electronic device based on these organic semiconductors.

Financial support of this work from the National Science Council, Taiwan, the Republic of China is gratefully acknowledged.

[1]V. C. Sundar, J. Zaumseil, V. Podzorov, E. Menard, R. L. Willett, T. Someya, M. E. Gershenson, and J. A. Rogers, Science **303**, 1644 (2004).
[2]J. Cornil, D. Beljonne, J.-P. Calbert, and J. L. Brédas, Adv. Mater. (Weinheim, Ger.) **13**, 1053 (2001); W. Q. Deng and W. A. Goddard III, J. Phys. Chem. B **108**, 8614 (2004).
[3]W. S. Hu, Y. F. Lin, Y. T. Tao, Y. J. Hsu, and D. H. Wei, Macromolecules **38**, 9617 (2005); W. S. Hu, S. Z. Weng, Y. T. Tao, H. J. Liu, H. Y. Lee, L. J. Fan, and Y. W. Yang, Langmuir **23**, 12901 (2007).
[4]W. S. Hu, Y. T. Tao, Y. J. Hsu, D. H. Wei, and Y. S. Wu, Langmuir **21**, 2260 (2005).
[5]M. J. Loiacono, E. L. Granstrom, and C. D. Frisbie, J. Phys. Chem. B **102**, 1679 (1998); D. Fichou, F. Charra, and A. O. Gusev, Adv. Mater. (Weinheim, Ger.) **13**, 555 (2001).
[6]T. W. Kelley, E. L. Granstrom, and C. D. Frisbie, Adv. Mater. (Weinheim, Ger.) **11**, 261 (1999); H. Yang, T. J. Shin, M. M. Ling, K. Cho, C. Y. Ryu, and Z. Bao, J. Am. Chem. Soc. **127**, 11542 (2005).
[7]E. Menard, A. Marchenko, V. Podzorov, M. E. Gershenson, D. Fichou, and J. A. Rogers, Adv. Mater. (Weinheim, Ger.) **18**, 1552 (2006).
[8]M. Zhang, Z. Hu, and T. He, J. Phys. Chem. B **108**, 19198 (2004).
[9]E. M. Muller and J. A. Marohn, Adv. Mater. (Weinheim, Ger.) **17**, 1410 (2005); T. Heim, K. Lmimouni, and D. Vuillaume, Nano Lett. **4**, 2145 (2004).
[10]T. W. Odom, J. Christopher Love, D. B. Wolfe, K. E. Paul, and G. M. Whitesides, Langmuir **18**, 5314 (2002).
[11]S. F. Alvarado, L. Rossi, P. Müller, P. F. Seidler, and W. Riess, IBM J. Res. Dev. **45**, 89 (2001).
[12]I. H. Campbell, S. Rubin, T. A. Zaxodzinski, J. D. Kress, R. L. Martin, D. L. Smith, N. N. Barashkov, and J. P. Ferraris, Phys. Rev. B **54**, R14321 (1996); B. Boer, A. Hadipour, M. M. Mandoc, T. Woudenbergh, and P. W. M. Bolm, Adv. Mater. (Weinheim, Ger.) **17**, 621 (2005).
[13]G. Heimel, L. Romaner, E. Zojer, and J. L. Brédas, Nano Lett. **7**, 932 (2007).
[14]K. Ihm, B. Kim, T. H. Kang, K. J. Kim, M. H. Joo, T. H. Kim, S. S. Yoon, and S. Chung, Appl. Phys. Lett. **89**, 033504 (2006).
[15]Y. Zheng, D. Qi, N. Chandrasekhar, X. Gao, C. Troadec, and A. T. S. Wee, Langmuir **23**, 8336 (2007).